(Received 27 August 2025, Accepted 22 October 2025, Scheduled 9 November 2025)

An AMC-Backed Miniaturized Dual-Band Circularly Polarized RFID Reader Antenna for IoT Applications

Deepak Kumar[1] and Naveen Jaglan[2, *]

[1] *Department of Electronics and Communication Engineering, Jaypee University of Information Technology, Solan, India*
[2] *Centre of Excellence in 5G Technology and IoT, Department of Electronics and Communication Engineering Netaji Subhas University of Technology, Sector-3, Dwarka, New Delhi, India*

ABSTRACT: This paper presents a 2.45 GHz/5.8 GHz circularly polarized RFID reader antenna based on an Artificial Magnetic Conductor (AMC) for detecting tagged objects in IoT applications. An efficient reader antenna is proposed to increase the interrogation distance and reduce the uncertainty in tag detection. The antenna consists of two dipole pairs printed on both sides of the substrate to operate at 2.45 GHz and 5.8 GHz, connected via feed delay lines in a cross-dipole configuration. The read range is further enhanced by a 5×5 AMC surface placed $0.042\lambda_0$ below the printed antenna, where λ_0 is the wavelength at the lower resonant frequency. The AMC backing results in a gain of 7.1 dBi at 2.45 GHz and 9.41 dBi at 5.8 GHz, improving the read range of the reader. Impedance bandwidth is also enhanced to 2.25–2.91 GHz for the 2.45 GHz band and 5.1–6.3 GHz for the 5.8 GHz band, reducing tag detection errors. The axial ratio bandwidth of the antenna is 2.18–2.99 GHz at 2.45 GHz and 5.27–5.88 GHz at 5.8 GHz, ensuring circular polarization over the operating bands.

1. INTRODUCTION

Smart devices with autonomous connectivity and Internet of Things (IoT) capabilities have become a requirement for modern intelligent systems. Consequently, the number of IoT-based smart devices is rapidly increasing [1], leading to significant growth in power consumption and spectrum usage. Backscatter communication provides a promising solution to this challenge.

Radio Frequency Identification (RFID) technology operates on the principle of backscatter communication, enabling data exchange between readers and tags without requiring additional power at the tag. The tags are energized solely by the RF signal emitted by the reader, which governs the entire object detection process. Therefore, each reader must be capable of handling multiple tags simultaneously, referred to as tag clusters [2]. This capability increases the reading range and improves tag detection probability, as fewer readers are required along the communication path.

RFID operates across several assigned frequency bands, including low frequency (LF) at 125–135 kHz, high frequency (HF) at 13.56 MHz, ultrahigh frequency (UHF) at 433.92 MHz and 860–960 MHz, and the Industrial, Scientific, and Medical (ISM) band at 2.45/5.8 GHz. With the rapid evolution of RFID technology, there is a growing demand for the 2.45/5.8 GHz bands due to their higher data transfer rates and longer reading range capabilities. The polarization and gain of an RFID antenna are critical parameters that directly influence its reading range [3]. While linearly polarized antennas can be effective, they require precise alignment between the reader and tag. Since tag orientation cannot always be guaranteed in practical scenarios, circular polarization is often preferred for reliable data transmission. Various techniques have been proposed in the literature to achieve circular polarization, including the addition of parasitic elements, corner truncation, and the use of cross-slots [4–9]. However, in terms of design simplicity and compact size, cross-dipole antennas with delay lines have proven to be an effective alternative for achieving circular polarization [8].

Despite their advantages, cross-dipole circularly polarized antennas, such as the design reported in [10], often suffer from low peak gain, limiting their effectiveness in long-range RFID applications. One effective approach to enhance antenna gain is the incorporation of metasurfaces, which not only improve gain but also promote a unidirectional radiation pattern, a critical requirement for RFID reader performance. Among them, artificial magnetic conductor (AMC) is an engineered metasurface designed to mimic properties of a perfect magnetic conductor (PMC), a theoretical construct not found in nature. AMC surfaces can reflect electromagnetic waves in phase, thereby enhancing antenna efficiency and directivity.

The use of AMCs has shown promising results in dual-band cross-dipole antenna designs, such as the configuration in [11], which employed a cross-slotted patch combined with a 5×5 AMC array. However, that design suffered from a large footprint, making it challenging to integrate into modern compact RFID reader systems and IoT devices, where miniaturization is crucial.

A single-band AMC-based compact antenna was reported in [12], which was not suitable for commercial applications. Considering the requirements for fast data rates and size con-

* Corresponding author: Naveen Jaglan (naveenjaglan1@gmail.com).

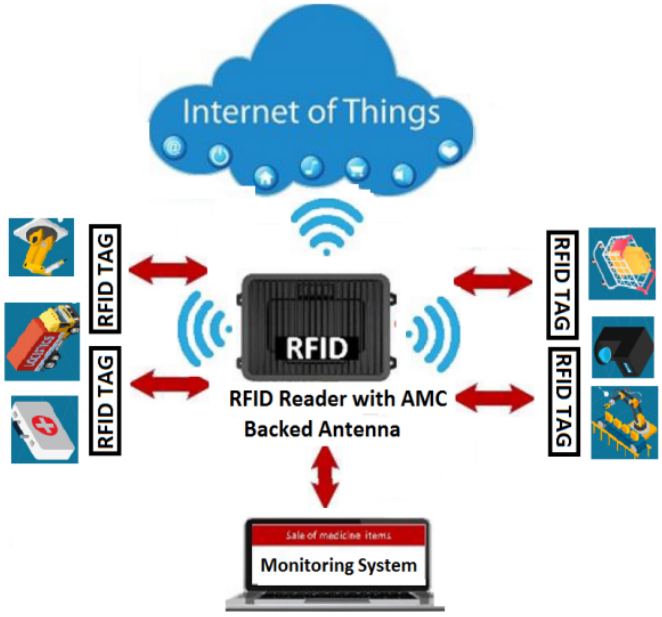

FIGURE 1. Illustration of RFID reader with IoT network.

straints, several 2.45/5.8 GHz AMC-backed antenna structures have been proposed [13–19]. For instance, a meandered-line coplanar waveguide (CPW)-fed antenna backed by a 5×6 AMC array was presented in [13]; however, this design was large and linearly polarized. A dual-polarized antenna with bow-tie patches and an AMC surface was reported in [14], increasing both antenna complexity and size. In [15], a large linearly polarized CPW-fed antenna with an 8×8 AMC array was proposed. A multiband CPW-fed antenna with an AMC surface incorporating a capacitor was presented in [16], which increased the cost and complexity of the reflector. Ref. [17] proposed a CPW antenna with a simple AMC design but with a large cross-sectional area. A compact dual-band antenna with an AMC reflector was reported in [10]; however, due to a smaller number of AMC elements, it suffered from reduced gain. In [18], a slotted patch antenna with an AMC array acting as a PMC at higher frequencies provided good gain but was linearly polarized. Similarly, [19] proposed a circularly polarized AMC-backed antenna with compact size, but the AMC array had a relatively large height.

These studies underscore the high demand for circularly polarized antennas that combine compact size, high gain, and wide impedance bandwidth. In this paper, we present a miniaturized circularly polarized cross-dipole RFID reader antenna with an AMC design operating at 2.45/5.8 GHz, specifically aimed at minimizing tag detection uncertainty in IoT networks. The proposed cross-dipole antenna consists of two dipole pairs printed on both sides of the substrate. The first dipole pair, with L-shaped arms arranged in a swastika-like configuration, excites the 2.45 GHz band, while the second dipole pair, composed of C-shaped elements, excites the 5.8 GHz band. Circular polarization is achieved using double delay lines in both frequency bands. The AMC unit cell consists of two concentric square rings: the outer ring with four orthogonal slits excites the 2.45 GHz band, while the smaller inner ring excites the 5.8 GHz band.

A 5×5 AMC array combined with delay lines enhances the proposed RFID antenna, improving both gain and reader range, making it highly suitable for IoT applications. Its dual-band operation, compact size, circular polarization, high gain, and energy efficiency further support reliable performance in IoT networks, as shown in Figure 1.

2. ANTENNA DESIGN

A circularly polarized antenna requires two orthogonal electric field components of equal amplitude and a 90° phase difference. A schematic configuration of the proposed cross-dipole antenna with orthogonally connected ring delay lines is illustrated in Fig. 2. For operation at the lower band (2.45 GHz), the dipole arm length is approximately $\lambda_{2.45\,\mathrm{GHz}}/4$, while the 90° phase delay line employing a concentric ring structure also has an effective length of $\lambda_{2.45\,\mathrm{GHz}}/4$. As shown in Fig. 2(a), right-hand circular polarization (RHCP) at 2.45 GHz is achieved by feeding one dipole arm directly through a coaxial line and the orthogonal arm through the 90° phase delay line. For the higher band (5.8 GHz), the dipole arm length is $\lambda_{5.8\,\mathrm{GHz}}/4$, as depicted in Fig. 2(b). Left-hand circular polarization (LHCP) at 5.8 GHz is realized by directly feeding one dipole arm and exciting the orthogonal arm via the 90° phase delay line. By integrating both dipole structures, a compact dual-band circularly polarized antenna capable of generating RHCP and LHCP at 2.45 GHz and 5.8 GHz, respectively, is obtained.

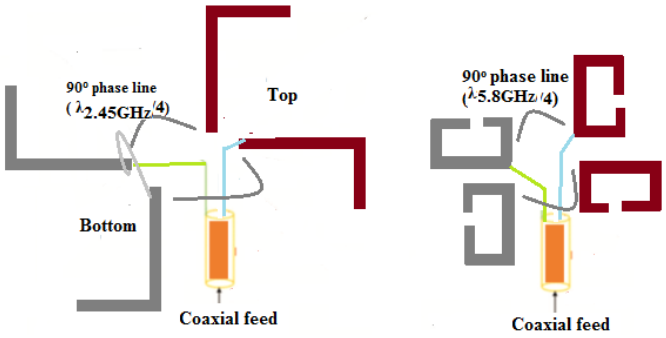

FIGURE 2. Representation of the feeding mechanism of the dual band circularly polarized antenna at (a) 2.45 GHz and (b) 5.8 GHz.

A detailed layout of the RFID reader antenna is presented in Fig. 3, which is fabricated on an FR4 substrate with a thickness (h) of 1.6 mm. The design parameters of the RFID reader antenna are listed in Table 1. In this study, orthogonal cross-dipole elements are incorporated on both sides of the substrate. The first dipole pair, featuring L-shaped arms arranged in a swastika-like configuration, is designed to excite the 2.45 GHz frequency band, whereas the second dipole pair, consisting of C-shaped elements, is intended to excite the 5.8 GHz frequency band. The antenna is simulated using High Frequency Structure Simulator (HFSS) software.

For RFID applications, the antenna must exhibit multi-band operation and circular polarization. However, most multi-band RFID antennas reported in the literature are linearly polarized, making it challenging to realize an antenna capable of operating at multiple resonant frequencies while maintaining circular

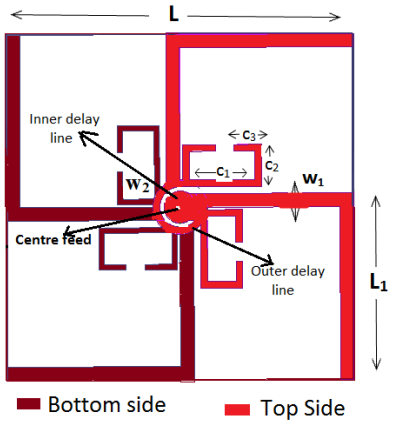

FIGURE 3. Top view Layout of proposed RFID antenna.

polarization. Cross-dipole configurations offer an effective solution to this limitation.

A typical cross-dipole antenna comprises radiating elements and delay lines. The length of each radiating element is approximately $\lambda_f/4$, where λ_f corresponds to the wavelength at the desired operating frequency. To achieve the required resonant frequency, orthogonal radiating elements are placed on both sides of the substrate. For multi-band performance, additional radiating elements are introduced. The delay lines, having a length of $\lambda_{2.45\,\mathrm{GHz}}/4$ (where $\lambda_{2.45\,\mathrm{GHz}}$ corresponds to the wavelength at the lower frequency band), are employed to generate a 90° phase shift necessary for circular polarization. By connecting the radiating dipole elements through these delay lines, a cross-dipole structure capable of multi-band circular polarization is realized.

The required frequency bands for the RFID reader antenna in IoT networks are 2.45 GHz and 5.8 GHz. The corresponding wavelengths are given by $\lambda_{2.45} = c/2.45 \times 10^9$ meters and $\lambda_{5.8} = c/5.8 \times 10^9$ meters, where c is the speed of light in m/s. The size of the radiating element for a 5.8 GHz frequency is given by:

$$L_1 + L/2 \approx \lambda_{4.5}/4 \tag{1}$$

The radiating elements size for the 2.45 GHz frequency is:

$$C_1 + 2C_2 + C_3 \approx \lambda_{5.8}/4 \tag{2}$$

The delay feed lines of proposed antenna is chosen as $\lambda_{2.45}/4$, which is circumference of outer delay line. The inner delay line has diameter, D, which is twice the width of the strip of the 2.45 GHz element W_1.

Figure 4 depicts the surface current distribution of the proposed antenna at 2.45 GHz. As shown in Fig. 4(a), the maximum current density is concentrated along the horizontal arms of the first dipole pair at $\theta = 0°$. When θ increases to 90°, the current maximum shifts to the vertical arms of the same dipole, as illustrated in Fig. 4(b). The surface current exhibits a counterclockwise rotation from $\theta = 0°$ to 270°, confirming that the proposed antenna radiates a right-hand circularly polarized (RHCP) wave at 2.45 GHz.

Figure 5 illustrates the surface current distribution of the proposed antenna at 5.8 GHz. As shown in Fig. 5(a), the maximum current density is concentrated along the C-shaped dipole elements at $\theta = 0°$, while an orthogonal shift in the current direction is observed at $\theta = 90°$, as depicted in Fig. 5(b). The surface current exhibits a counterclockwise rotation from $\theta = 0°$ to 270°, indicating that the antenna radiates a right-hand circularly polarized (RHCP) wave at 5.8 GHz.

TABLE 1. Detailed dimensions of the proposed antenna.

Parameter	*(mm)*	*Parameter*	*(mm)*	*Parameter*	*(mm)*
L	24	R_1	2.55	P_1	14.2
L_1	12	R_2	1.21	P_2	9.27
C_1	6	W_1	1	W	42
C_2	2.7	W_2	0.4	R	1.9
C_3	1.2	P	14.4	g_1	1.74
t_1	1.79	t_2	1.63	L_A	72
H	5	h	1.6	ε_r	4.4

The feed delay lines have important role in optimizing antenna parameters. The effect of delay line on impedance bandwidth and axial ration of proposed RFID reader is shown in Fig. 6 and Fig. 7. Fig. 6(a) shows the effect of delay lines on bandwidth.

3. AMC DESIGN AND INTEGRATION WITH RFID ANTENNA

As discuss previously, an AMC can be used to improve the tag detection probability of RFID reader. This AMC increases the antenna gain and achieve unidirectional radiation pattern from the reader. The designed AMC unit cell on an FR4 substrate is shown in Fig. 8. The AMC unit cell features two concentric square rings to achieve the 2.45 GHz and 5.8 GHz frequencies. The outer square ring, which has a longer length and four orthogonal slits, excites the 2.45 GHz frequency, while the smaller inner square ring excites the 5.8 GHz frequency.

An AMC reflector is placed below the radiating surface to improve the antenna performance. The AMC surface works as a filter tuned to desired frequency band. Its good filtering ability lowers the uncertainty of tag detection.

AMC reflectors are artificially designed materials having negative refractive index, defined as:

$$n = -\sqrt{\varepsilon\mu}, \quad \text{€}R, n < 0 \tag{3}$$

The AMC have low permittivity and higher permeability, which allow the magnitude of wave impedance to approach infinity. Wave impedance of AMC is defined as the ratio of the magnitude of the electric field to the magnitude of the magnetic field. To relate this with the main mechanism of reflection at the AMC boundary, the reflection and transmission coefficients are related as given below

$$S_{11} = \frac{\eta - \eta_0}{\eta + \eta_0} \frac{1 - e^{-2jkd}}{1 - \left[\eta - \frac{\eta_0}{\eta} + \eta_0\right]^2 e^{-2jkd}} \tag{4}$$

$$S_{21} = \frac{4\eta\eta_0}{\eta + \eta_0} \frac{e^{-2jkd}}{1 - \left[\eta - \frac{\eta_0}{\eta} + \eta_0\right]^2 e^{-2jkd}} \tag{5}$$

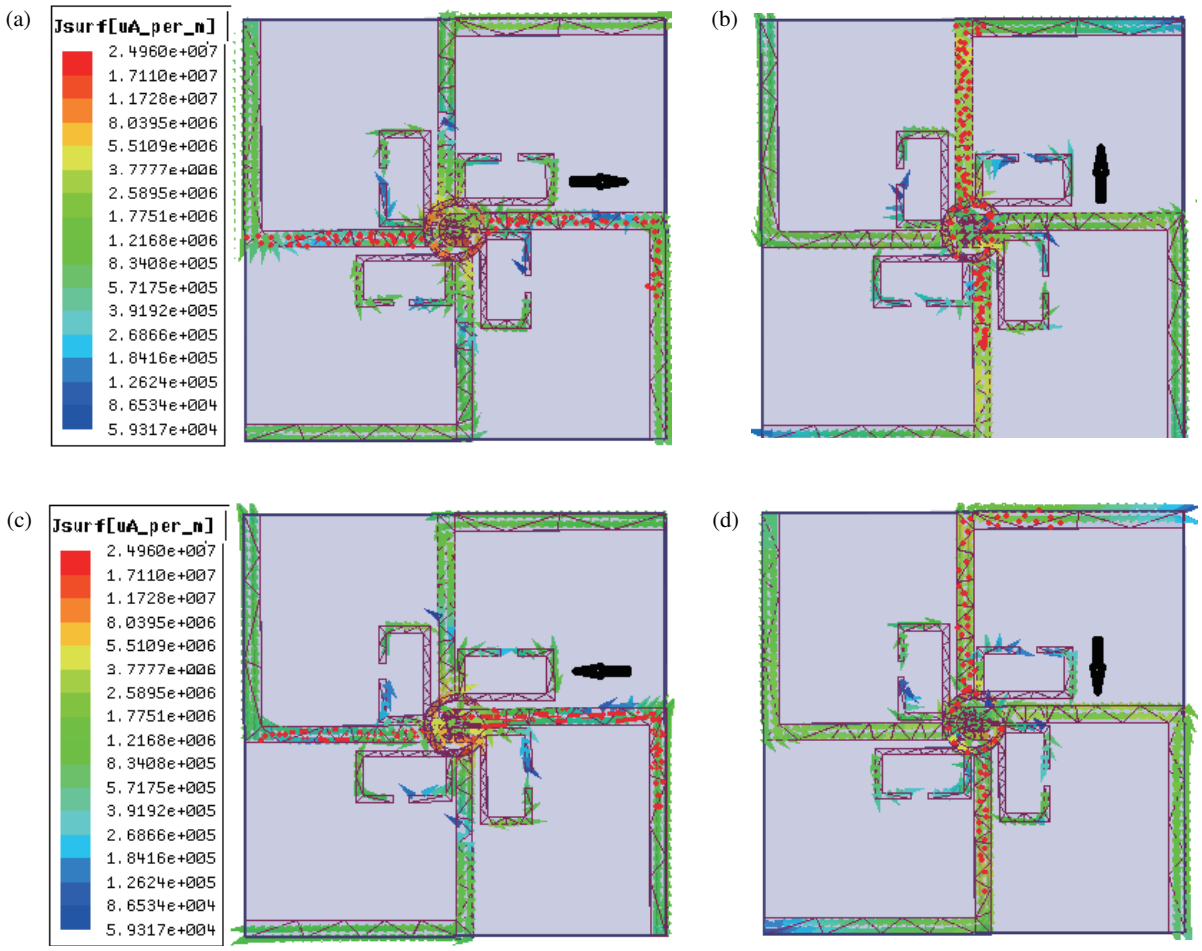

FIGURE 4. Current distribution at 2.45 GHz (a) $\theta = 0°$, (b) $\theta = 90°$ (c) $\theta = 180°$ (d) $\theta = 270°$.

where $\eta = \frac{E_x}{H_Y}$, $E_x(x, y, z) = Ae^{-jkz}$ and, $E_y(x, y, z) = \frac{A}{\eta_0}e^{-jkz}$. And $\eta_0 \to \infty$, the desired reflection with zero-degree phase occurs as follows:

$$\lim_{|n|\to\infty} S_{11} = +1, \quad \text{and} \quad \lim_{|n|\to\infty} S_{21} = 0 \tag{6}$$

The zero-degree phase reversal in the case of AMC reflectors is shown in Equation (6). The AMC structure forms a Fabry-Perot cavity due to ground plane, which excites maximum current at the desired resonant frequency. At this point the generated current is out of phase with the incident wave. This yields a reflectivity of $+1$ and a phase reversal of 0°. The reflection mechanism of incident wave from AMC surface is shown in Fig. 9.

When incident wave is struck by an incident wave from the antenna, the AMC layer produces a backward wave. The reflected wave adds constructively to the antenna radiation, increasing the antenna gain.

The AMC unit cell is arranged in a 5×5 array and positioned underneath the cross-dipole antenna at a height of H as shown in Fig. 10. Each AMC unit cell measures 14.4 mm $\times$ 14.4 mm, resulting in an overall AMC array size of 72 mm $\times$ 72 mm. The AMC layer acts as a reflector, reflecting the 2.4 GHz and 5.8 GHz frequency waves while absorbing signal at other frequencies, thereby enhancing the antenna's performance. This AMC reflector layer also reduces back radiation resulting in increased antenna gain.

Fig. 11(a) illustrates the effect of parameter H on the reflection coefficient of AMC-backed antenna. The impedance bandwidths in both the bands are narrow for $H = 3$ mm whereas for $H = 7$ mm, impedance matching is good in 2.45 GHz but deteriorates in 5.8 GHz. Therefore $H = 5$ mm is considered for the antenna design as it provides better impedance matching in both bands. The reflection coefficients of proposed antenna with different (3×3, 5×5, 7×7) AMC arrays are depicted in Fig. 11(b). It can be observed that as the array size increases, the impedance matching varies in the 2.45 GHz band whereas 5.8 GHz band shifts to a higher frequency as the array size increases from 3×3 to 7×7. However, overall good impedance at desired bands is obtained for 5×5 AMC array size.

The size of the used AMC is also important as it determines the total size of the proposed antenna. Thus, the array size increasing from 3×3 to 5×5 results in a significant increase in gains which indicates that the overall size increase is useful. However, when array size is increased from 5×5 to 7×7, the increase in gain is very small, despite the significant increase in overall size. Therefore, 5×5 is most appropriate array size for

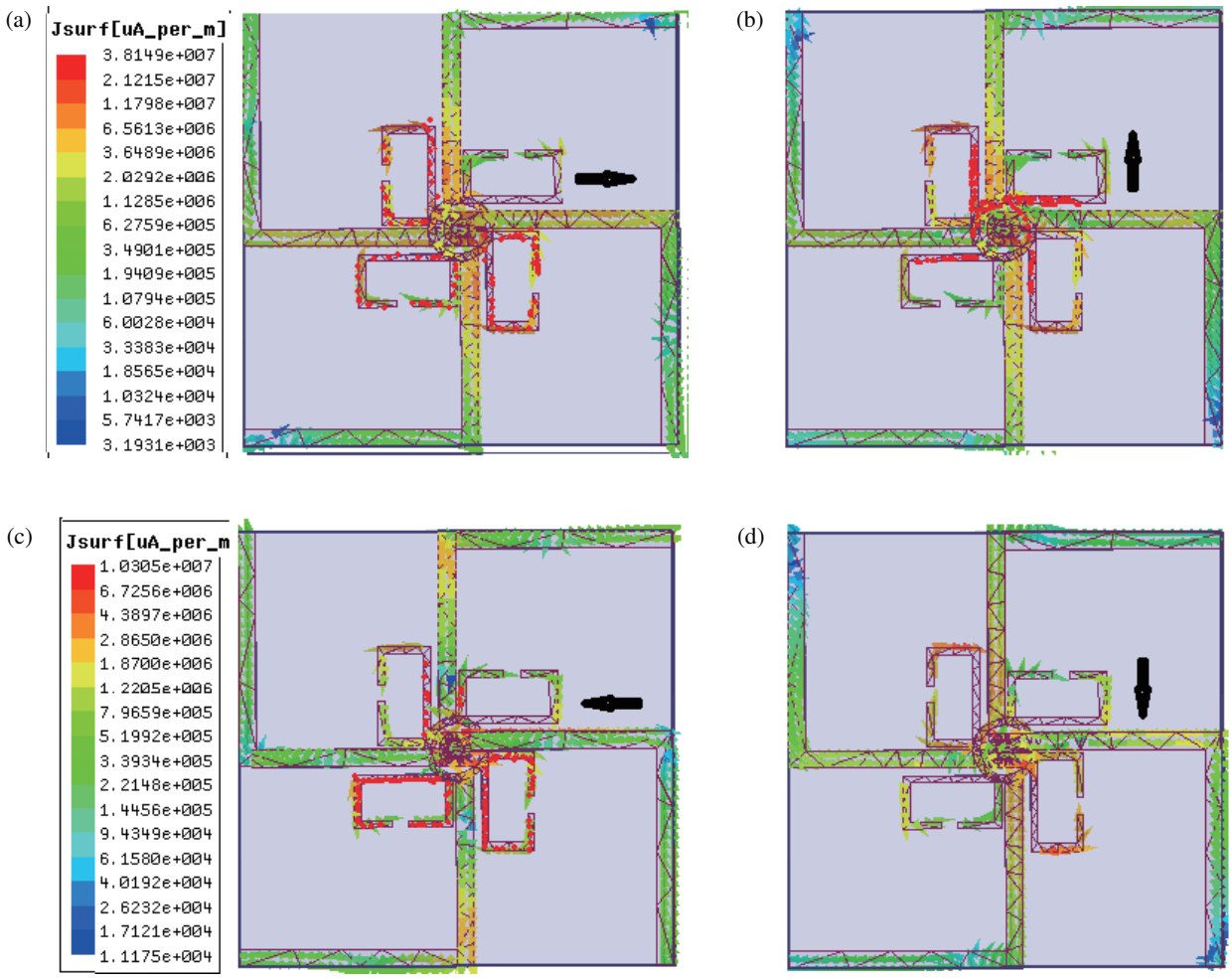

FIGURE 5. Current distribution at 5.8 GHz (a) $\theta = 0^{\circ}$, (b) $\theta = 90^{\circ}$ (c) $\theta = 180^{\circ}$ (d) $\theta = 270^{\circ}$.

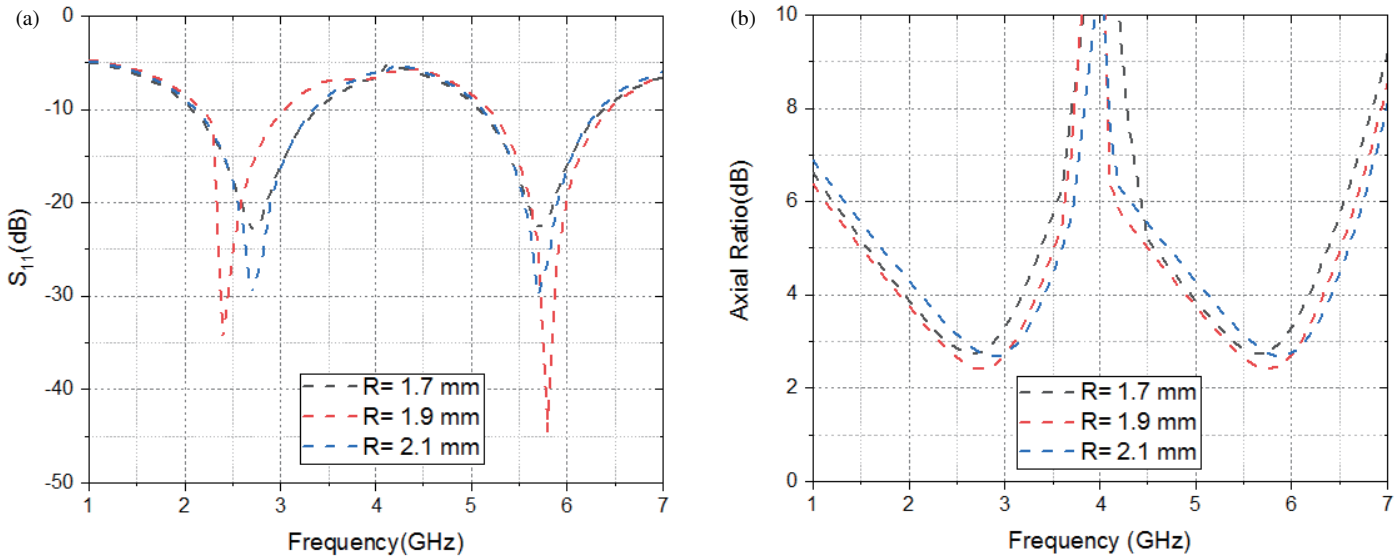

FIGURE 6. (a) Effect of delay line radius on impedance bandwidth. (b) Effect of axial ratio on variation of delay line radius.

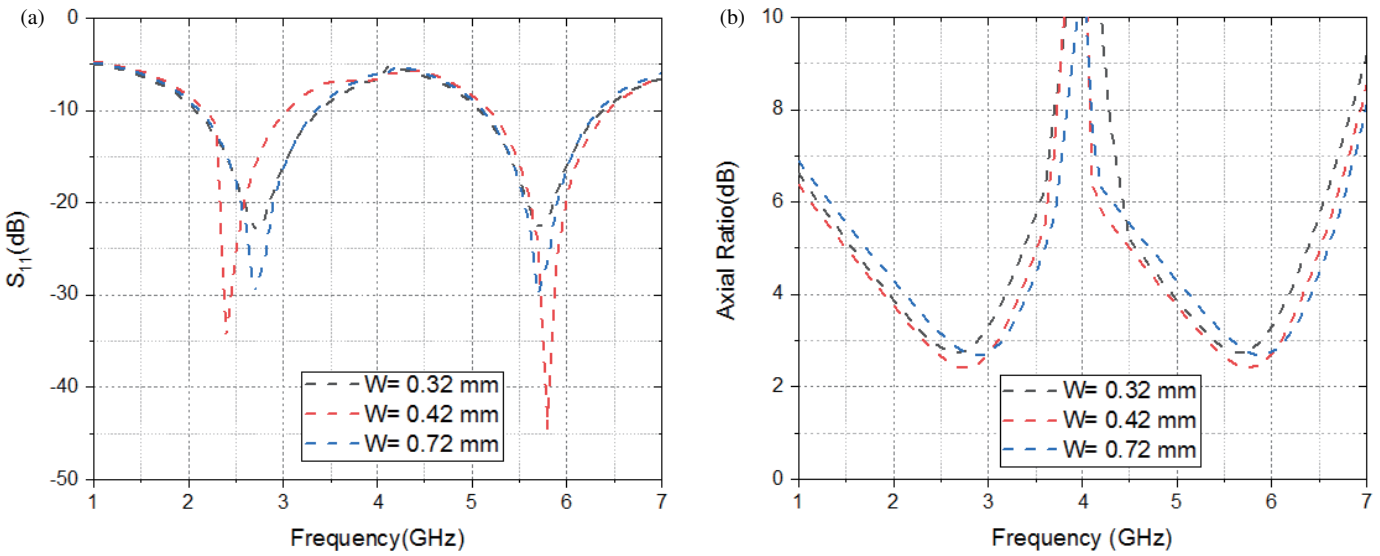

FIGURE 7. (a) Effect of feed delay line width on S_{11} bandwidth. (b) Effect of feed delay line width on axial ratio.

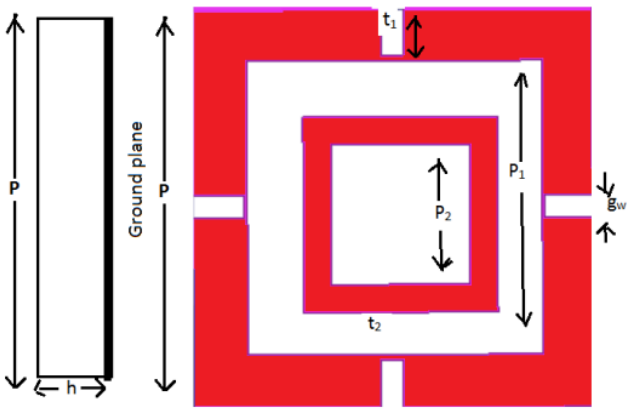

FIGURE 8. Layout of AMC unit cell.

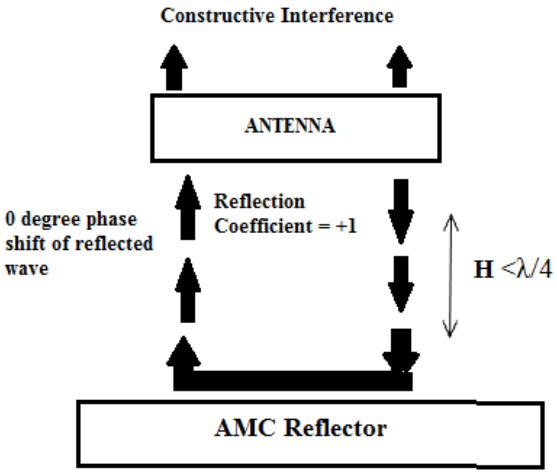

FIGURE 9. Mechanism of reflection of incident wave from antenna.

the proposed antenna configuration in order to achieve higher antenna gain with compact size.

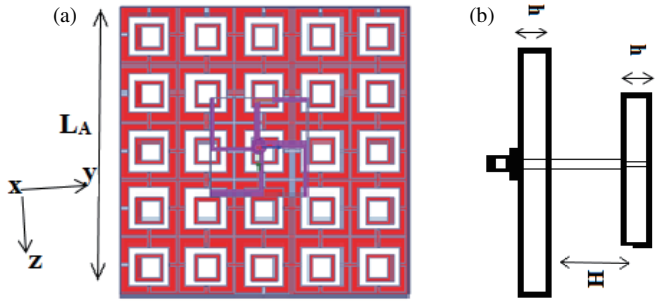

FIGURE 10. Arrangement reader antenna with a 5 × 5 AMC array. (a) Top view. (b) Side view.

Fig. 12 shows the reflection coefficients of the cross-dipole antenna with and without the AMC layer. The return loss value changes from −25 dB to −35 dB at 2.45 GHz and from −30 dB to −45 dB at 5.8 GHz.

4. RESULTS AND DISCUSSION

4.1. Antenna Measurement

The proposed 5 × 5 AMC-backed RFID reader antenna was fabricated and experimentally tested to validate its performance. Photographs of the fabricated prototypes are shown in Figs. 13(a)–(c). The measured reflection coefficient (S_{11}) of the AMC-backed RFID reader antenna is presented in Fig. 14(a).

4.2. Performance Evaluation

As shown in Fig. 14(a), the simulated impedance bandwidths of the proposed antenna with the AMC backing are 2.25–2.91 GHz for the 2.45 GHz band and 5.1–6.3 GHz for the 5.8 GHz band. The measured impedance bandwidths of the

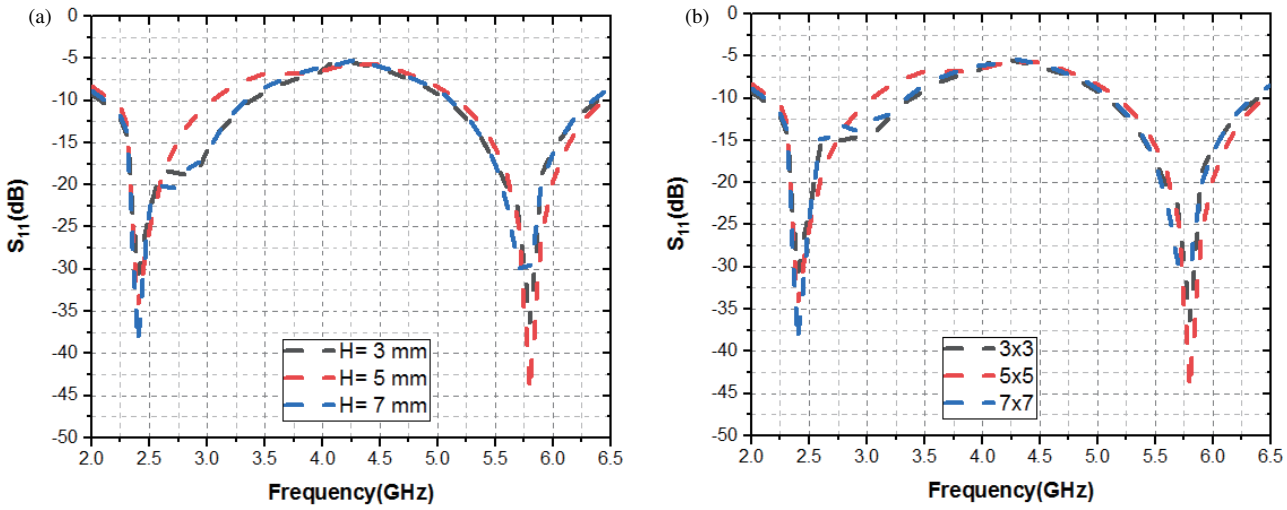

FIGURE 11. Effect of the parameter H and AMC arrays on the reflection coefficient (a) H, (b) AMC arrays.

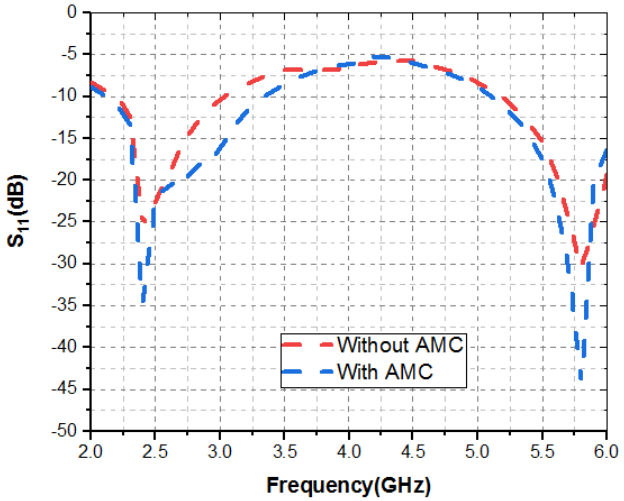

FIGURE 12. Reflection coefficient with and without AMC arrays.

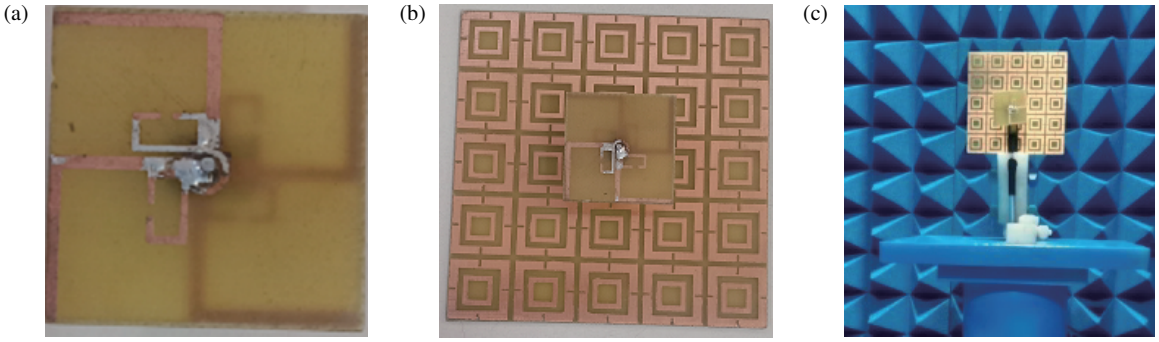

FIGURE 13. Fabricated antenna. (a) Top view without AMC. (b) antenna with AMC design. (c) Measurement in anechoic chamber.

fabricated prototype are 2.16–2.94 GHz and 5.2–6.1 GHz for the 2.45 GHz and 5.8 GHz bands, respectively.

The simulated axial ratio bandwidths are 2.25–2.98 GHz and 5.4–5.9 GHz whereas the measured axial ratio bandwidths are 2.18–2.99 GHz and 5.27–5.88 GHz in the 2.45 GHz and 5.8 GHz bands respectively are presented in Fig. 14(b).

The simulated peak gains at 2.45 GHz and 5.8 GHz are 7.1 dBi and 9.41 dBi, respectively, whereas the measured peak gains of this antenna are 6.45 dBi and 8.5 dBi in the 2.45 GHz

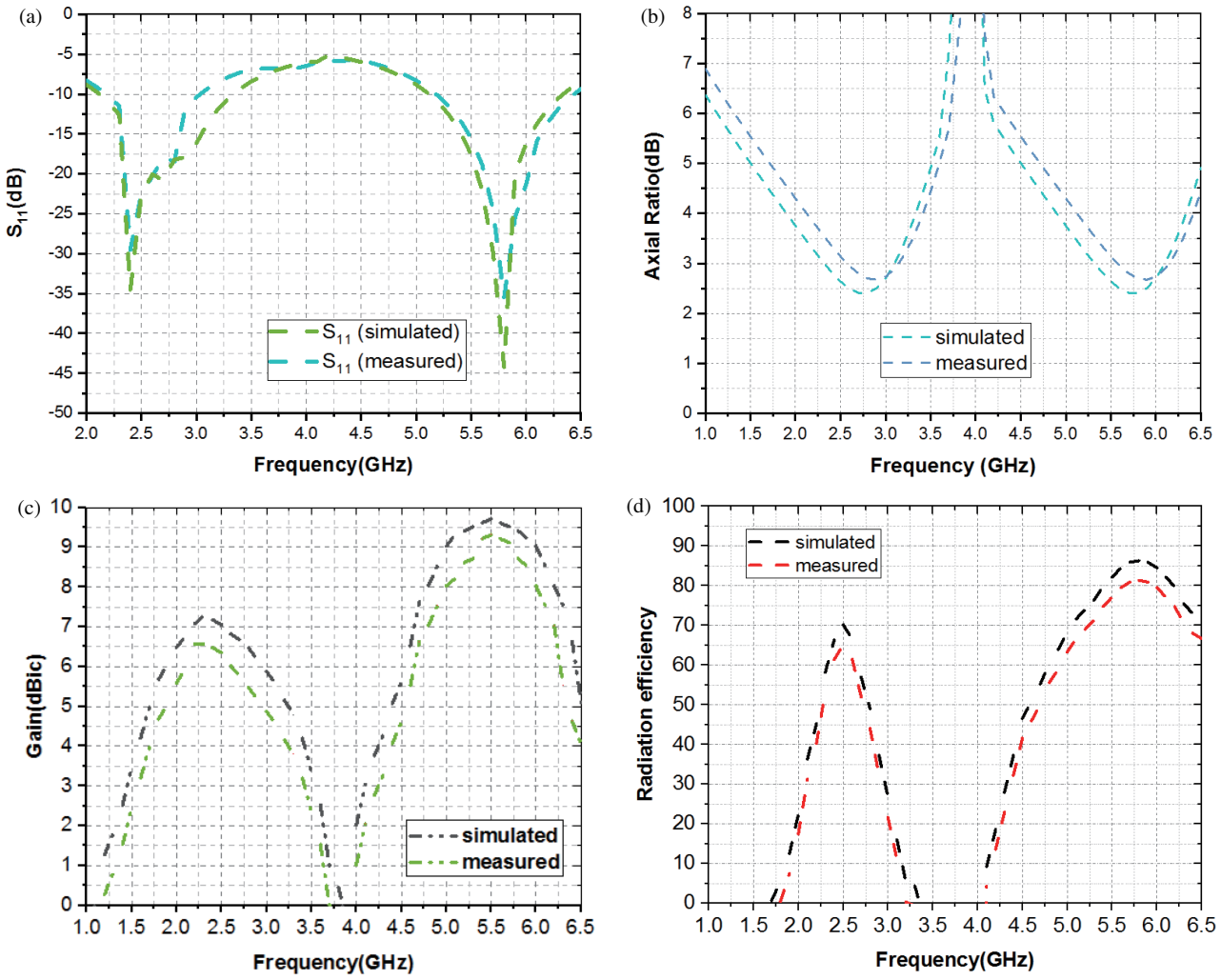

FIGURE 14. (a) Simulated and measured reflection coefficients. (b) Simulated and measured axial bandwidths. (c) Simulated and measured peak gains. (d) Simulated and measured radiation efficiencies.

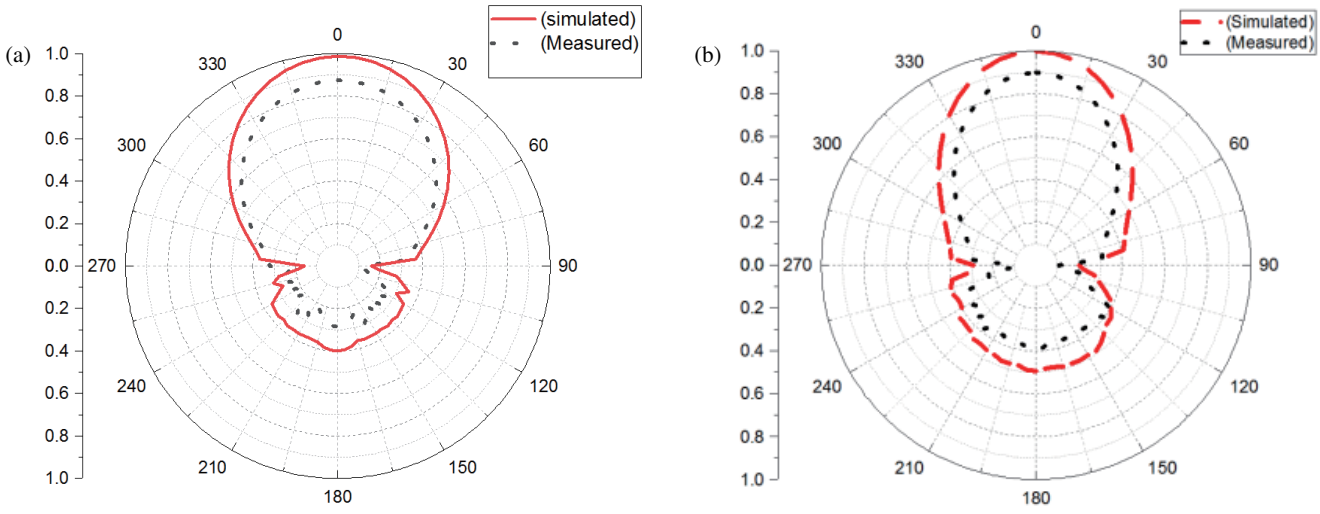

FIGURE 15. Radiation patterns at (a) 2.45 GHz (b) 5.8 GHz.

TABLE 2. Comparison with existing literature.

Ref.	*Pol.*	S_{11} *(GHz)(sim.)*	*Axial Ratio (GHz)(sim.)*	*Peak Gain (dBi)(sim.)*	*Antenna Size (mm × mm)*	*AMC Unit cell Size (mm × mm*	*AMC Array*	*AMC Array Size (mm × mm)*	*Total height (mm)*
[13]	CP	(0.74–1.1), (2–3.05)	0.77–1.06 2.22–2.95	9.1; 15.2	104 × 104	30 × 30	10 × 10	300 × 300	39.52
[14]	CP	(0.903–0.927), (2.42–2.27)	0.902–0.95 2.423–2.47	3.1; 6.2	100 × 100	42 × 42	5 × 5	210 × 210	33.2
[15]	LP	(2.36–2.76), (2–3.05)	-	9.1; 15.2	104 × 104	30 × 30	10 × 10	300 × 300	39.52
[16]	LP	(2.3–3), (5.1–6.2)	-	8.6; 3.7	120 × 120	18 × 18	8 × 8	144 × 144	13
[17]	LP	(2.13–2.87), (5.54–5.86)	-	5.29; 6.7	37.26 × 28.17	18 × 18	5 × 5	90 × 90	26.2
[10]	LP	(2.32–2.45), (5.37–5.71)	-	5.2; 7.7	25 × 30	24 × 24	3 × 3	72 × 72	5
[18]	LP	(2.41–2.51), (5.72–5.85)	-	6.43; 7.75	25 × 35	19.7 × 19.7	3 × 3	59.1 × 59.1	4.1
[19]	CP	(2.32–2.57), (5.48–6)	2.385–2.485, 5.77–5.88	6.1; 7.9	25 × 25	14.4 × 14.4	5 × 5	72 × 72	8.2
Prop.	CP	(2.25–2.91), (5.1–6.3)	2.18–2.99, 5.27–5.88	7.1, 9.41	24 × 24	14.2 × 14.2	5 × 5	72 × 72	8.2

Pol = Polarization, LP = Linear Polarization, CP = Circular Polarization, mm = millimeter, dB = decibel, sim-Simulated

and 5.8 GHz bands, respectively, illustrated in Fig. 14(c). Fig. 14(d) shows efficiencies of the AMC backed antenna.

The simulated radiation efficiencies in 2.45 GHz and 5.8 GHz are 70.1% and 87.7%, respectively, whereas measured values of radiation efficiencies are 65.4% and 82.1% in the 2.45 GHz and 5.8 GHz bands, respectively.

The radiation patterns of antenna with AMC at 2.45 GHz and 5.8 GHz frequencies are shown in Fig. 15. It can be observed that the radiation patterns become more unidirectional due to the inclusion of AMC reflector, making it well-suited for the use in RFID readers.

5. PERFORMANCE COMPARISON

The comparison of various existing AMC backed RFID reader antennas based on parameters such as impedance bandwidth, peak gain, size, AMC unit cell, and array size are shown in Table 2. The antennas in [13, 14] had good impedance bandwidths and peak gains, but they were large in size due to large AMC array. These AMC arrays had large number of unit cells with large size resulting in large configurations. The antennas in [15–17] were relatively compact in size, but are linearly polarized. In [18], the metasurface-backed antenna employs relatively simple AMC layers to enhance gain or enable a low-profile design for linearly polarized bands. However, such implementations often exhibit moderate radiation efficiency and require comparatively large antenna and AMC dimensions. More advanced metasurface-backed designs [19] utilize multi-resonant unit cells, tailored reflection phase characteristics, and polarization conversion mechanisms to achieve improved performance and compactness. These strategies enable two independently tunable circularly polarized (CP) resonances, achieving dual-band CP operation while maintaining or enhancing radiation efficiency through optimized impedance matching and a compact antenna — AMC configuration.

As discussed previously, circularly polarized antennas are highly desirable for RFID readers due to their increased read range and improved tag detection accuracy.

In the proposed design, multi-resonant unit cells with slits forming two concentric square rings are employed to achieve operation at 2.45 GHz and 5.8 GHz. The outer square ring, with a larger perimeter and four orthogonal slits, excites the 2.45 GHz resonance, while the smaller inner square ring excites the 5.8 GHz resonance. This configuration enables dual-band operation with enhanced radiation efficiency and a compact overall size. Thus, the proposed antenna achieves a compact form factor with a 5×5 AMC surface.

6. CONCLUSION

This research paper presents a miniaturize dual band 2.45 GHz/5.8 GHz circularly polarized Artificial Magnetic conductor (AMC) based RFID reader antenna to detect tagged objects for IoT application. Here an efficient reader antenna is presented to increase the interrogation distance of the reader and decrease the uncertainty of tagged object detection. The proposed RFID antenna consists of two dipole pairs printed on both sides of the substrate to obtain 2.45 GHz and 5.8 GHz bands connected by feed delay lines with cross dipole arrangement.

The first dipole pair, featuring L-shaped arms arranged in a swastika-like configuration, is designed to excite the 2.45 GHz frequency band, while the second dipole pair, consisting of C-shaped elements, is intended to excite the 5.8 GHz frequency band. Circular polarization is achieved by incorporating double delay lines in both frequency bands. The AMC unit cell consists of two concentric rings. The outer ring with four orthogonal slits excites the 2.45 GHz band while the smaller inner ring excites the 5.8 GHz band.

The range of RFID reader antenna is improved by 5 × 5 AMC surface placed $0.042\lambda_0$ below the printed antenna (where λ_0 is wavelength at the lowest resonant frequency). The AMC backing RFID reader antenna had the gain of 7.1 dBi at 2.5 GHz and 9.41 dBi at 5.8 GHz, respectively. This also enhanced the read range of reader. There is also improvement in impedance bandwidth 2.25–2.91 GHz in the 2.45 GHz band and 5.1–6.3 GHz in the 5.8 GHz band which reduces tag detection error. The axial ratio bandwidth of the antenna configuration is 2.18–2.99 GHz in the 2.45 GHz and 5.27–5.88 GHz in 5.8 GHz band, respectively. The measured results align well with the simulated ones, indicating that the proposed RFID reader antenna, with its compact size, circular polarization, and enhanced reading range is well-suited for IoT application.

REFERENCES

[1] Xue, F., Y. Zhang, J. Li, and H. Liu, "Circularly polarized cross-dipole antenna for UHF RFID readers applicated in the warehouse environment," *IEEE Access*, Vol. 11, 38 657–38 664, 2023.

[2] Ji, B., K. Song, C. Li, W.-p. Zhu, and L. Yang, "Energy harvest and information transmission design in internet-of-things wireless communication systems," *AEU — International Journal of Electronics and Communications*, Vol. 87, 124–127, Apr. 2018.

[3] Xu, J., Z. Li, K. Zhang, J. Yang, N. Gao, Z. Zhang, and Z. Meng, "The principle, methods and recent progress in RFID positioning techniques: A review," *IEEE Journal of Radio Frequency Identification*, Vol. 7, 50–63, 2023.

[4] Kumar, D. and N. Jaglan, "A dual band circularly polarized RFID reader antenna for Internet of Things application," in *2023 9th International Conference on Signal Processing and Communication (ICSC)*, 13–16, NOIDA, India, 2023.

[5] Kumar, D., N. Jaglan, and S. D. Gupta, "A UHF RFID reader antenna design for retail self-billing application," in *2021 7th International Conference on Signal Processing and Communication (ICSC)*, 6–10, Noida, India, 2021.

[6] Xu, R. and Z. Shen, "Dual-band circularly polarized RFID reader antenna with combined dipole and monopoles," *IEEE Transactions on Antennas and Propagation*, Vol. 71, No. 12, 9593–9600, Dec. 2023.

[7] Birwal, A., K. Patel, and S. Singh, "Circular slot-based microstrip circularly polarized antenna for 2.45-GHz RFID reader applications," *IEEE Journal of Radio Frequency Identification*, Vol. 8, 10–18, 2024.

[8] Bajaj, C., D. K. Upadhyay, S. Kumar, and B. K. Kanaujia, "Compact circularly polarized cross dipole antenna for RFID handheld readers/IoT applications," *AEU — International Journal of Electronics and Communications*, Vol. 155, 154343, Oct. 2022.

[9] Gong, Y., S. Yang, B. Li, Y. Chen, F. Tong, and C. Yu, "Multiband and high gain antenna using AMC ground characterized with four zero-phases of reflection coefficient," *IEEE Access*, Vol. 8, 171 457–171 468, 2020.

[10] Ahmad, S., K. N. Paracha, Y. A. Sheikh, A. Ghaffar, A. D. Butt, M. Alibakhshikenari, P. J. Soh, S. Khan, and F. Falcone, "A metasurface-based single-layered compact AMC-backed dual-band antenna for off-body IoT devices," *IEEE Access*, Vol. 9, 159 598–159 615, 2021.

[11] Luo, Q., H. Tian, Z. Huang, X. Wang, Z. Guo, and Y. Ji, "Unidirectional dual-band CPW-fed antenna loaded with an AMC reflector," *International Journal of Antennas and Propagation*, Vol. 2013, No. 1, 875281, 2013.

[12] Su, Q., P. Yin, Y. Cheng, and L. Chen, "A low RCS microstrip antenna based on AMC metasurface," in *2023 IEEE International Symposium On Antennas And Propagation (ISAP)*, 1–2, Kuala Lumpur, Malaysia, 2023.

[13] Xu, R., J. Liu, K. Wei, W. Hu, Z.-J. Xing, J.-Y. Li, and S. S. Gao, "Dual-band circularly polarized antenna with two pairs of crossed-dipoles for RFID reader," *IEEE Transactions on Antennas and Propagation*, Vol. 69, No. 12, 8194–8203, Dec. 2021.

[14] Sarkar, S. and B. Gupta, "A dual-band circularly polarized antenna with a dual-band AMC reflector for RFID readers," *IEEE Antennas and Wireless Propagation Letters*, Vol. 19, No. 5, 796–800, May 2020.

[15] Zhai, H., K. Zhang, S. Yang, and D. Feng, "A low-profile dual-band dual-polarized antenna with an AMC surface for WLAN applications," *IEEE Antennas and Wireless Propagation Letters*, Vol. 16, 2692–2695, 2017.

[16] Dey, A., S. Bhattacharjee, S. R. B. Chaudhuri, and M. Mitra, "A dual band flexible antenna on AMC ground for wearable applications," in *2019 IEEE Asia-Pacific Microwave Conference (APMC)*, 607–609, Singapore, 2019.

[17] Wang, M., Z. Yang, J. Wu, J. Bao, J. Liu, L. Cai, T. Dang, H. Zheng, and E. Li, "Investigation of SAR reduction using flexible antenna with metamaterial structure in wireless body area network," *IEEE Transactions on Antennas and Propagation*, Vol. 66, No. 6, 3076–3086, Jun. 2018.

[18] Yin, B., M. Ye, Y. Yu, and J. Gu, "A dual-band miniaturized AMC-based wearable antenna for health monitoring applications," *Progress In Electromagnetics Research C*, Vol. 112, 165–177, 2021.

[19] Bajaj, C., D. K. Upadhyay, S. Kumar, and B. K. Kanaujia, "Directional energy-efficient metasurface-backed RFID reader antenna for minimizing tag-detection uncertainty in IoT networks," *IEEE Journal of Radio Frequency Identification*, Vol. 8, 88–97, 2024.